

Elasto-Plastic Analysis of Structural Problems Using Atomic Basis Functions

V. Kozulić¹ and B. Gotovac¹

Abstract: The numerical model for the elasto-plastic analysis of prismatic bars subjected to torsion is developed. The functions implemented in this model are Fup basis functions which belong to the class of atomic functions. The collocation method is used to form a system of equations in which the differential equation of the problem is satisfied in collocation points of closed domain, while boundary conditions are satisfied exactly at the domain boundary. The propagation of plastic zones in the cross-section is monitored by applying the incremental-iterative procedure until failure. An approximate solution of arbitrary accuracy is attained by hierarchically increasing the number of basis functions during non-linear calculation (multilevel approach) in places where plastic yielding occurs. The results obtained by the proposed method are compared with the existing exact solutions and numerical solutions obtained by the Finite Element Method. It can be concluded that the presented numerical model efficiently simulates the real non-linear behavior of the structure and provides excellent results for the elaborated problems.

Keywords: torsion problem of prismatic bars, plastic failure, atomic basis functions, universality, collocation method, multilevel base.

1 Introduction

The most widely used methods for numerical analysis of structural problems are finite difference, finite element and boundary element methods. A strong contender to complement the mesh-based methods is a newly emerging family of so-called meshless or meshfree methods for solving PDEs. The problems particularly suited for a meshfree solution approach are those posing major difficulties to the mesh-based methods: for example, problems involving large local gradients and singularities, multi-scale problems, strongly nonlinear problems, etc. Various meshless methods for solving the elastic torsion problems were developed by many authors.

¹ University of Split, Faculty of Civil Engineering, Architecture and Geodesy, 21000 Split, Croatia

Among them, numerical methods for obtaining solutions of the elastic torsion problem with complicated shapes of the cross-section are very interesting [Liu (2007)]. In this paper, we study the problem of elasto-plastic torsion of prismatic bars. Solving of non-linear engineering problems, in distinction from linear analyses, requires more complex numerical tool and therefore, larger number of numerical operations. For example, in elasto-plastic analyses it is interesting to detect plasticized zones and monitor their propagation parallel with the increase of load. In numerical procedures based on the weak formulation, plastic failure always records before it really happens. This is the consequence of the fact that the yielding criterion [Hill (1985)] is not tested in the same points in which displacements are calculated. More efficient solution of non-linear problems can be obtained by applying the procedure of the strong formulation with an arbitrary increase in the number of basis functions on the domain.

In the numerical modeling of elasto-plastic behaviour of prismatic bars subjected to torsion, we implemented the Fup basis functions which belong to the class of atomic functions [Rvachev and Rvachev (1971); Kravchenko, Rvachev, and Rvachev (1995)]. This is the first use of atomic basis functions in elasto-plastic analysis of the torsion problem. These basis functions possess the characteristics of practical application of splines (compact support) and, at the same time, the property of universality [Gotovac and Kozulić (1999)] which is a characteristic of algebraic and trigonometric polynomials. Because of the property of universality, it is possible to hierarchically increase the number of basis functions during non-linear calculation (multilevel approach). We created numerical model by applying the collocation method and incremental-iterative procedure for monitoring the propagation of plastic zones in the cross-section.

This paper is divided into six sections including this introduction. Section 2 presents a short description of the main features of the Fup basis functions. Section 3 gives the governing equations of the torsion problem and mathematical description of particular steps in the incremental-iterative procedure for non-linear analysis. The numerical model created by using Fup functions and collocation technique (Fup Collocation Method) is explained in Section 4. In Section 5 the new method is illustrated on some examples and obtained results are compared with the existing exact solutions and numerical solutions obtained by the FEM. Finally, we give a summary and conclusions in Section 6.

2 Fup basis functions

Fup basis functions belong to a class of atomic functions which are infinitely-differentiable functions with compact support [Rvachev and Rvachev (1971); Go-

tovac and Kozulić (1999)]. Atomic functions $y(\cdot)$ are defined as solutions of differential functional equations of the following type:

$$Ly(x) = \lambda \sum_{k=1}^M C_k y(ax - b_k) \quad (1)$$

where L is a linear differential operator with constant coefficients, λ is a nonzero scalar, C_k are coefficients of the linear combination, $a > 1$ is a parameter that defines the length of the compact support, and b_k are coefficients that determine displacements of the basis functions. Rvachev and Rvachev (1971), in their pioneering work, called these basis functions “atomic” because they span the vector spaces of all three fundamental functions in mathematics: algebraic, exponential and trigonometric polynomials. Also, atomic functions can be divided into an infinite number of smaller pieces that maintain all their properties, implying a so-called “atomic structure.”

The simplest function, which is the most-studied of the atomic basis functions, is the $up(x)$ function, Fig. 1. The function $up(x)$ is a smooth function with compact support over $[-1,1]$, which is obtained as a solution of a differential functional equation

$$up'(x) = 2 up(2x + 1) - 2 up(2x - 1) \quad (2)$$

with the normalized condition $\int_{-\infty}^{\infty} up(x) dx = \int_{-1}^1 up(x) dx = 1$. The function $up(x)$ can be expressed as an inverse Fourier transform:

$$up(x) = \frac{1}{2\pi} \int_{-\infty}^{\infty} e^{itx} \prod_{j=1}^{\infty} \left(\frac{\sin(t 2^{-j})}{t 2^{-j}} \right) dt. \quad (3)$$

Since Eq. 3 represents an exact but mathematically-intractable expression, Rvachev (1982) and Gotovac and Kozulić (1999) provided a numerically more-adequate expression for calculating the function $up(x)$:

$$up(x) = 1 - \sum_{k=1}^{\infty} (-1)^{1+p_1+\dots+p_k} p_k \sum_{j=0}^k C_{jk}(x - 0, p_1 \dots p_k)^j \quad (4)$$

where coefficients C_{jk} are rational numbers determined according to the following expression:

$$C_{jk} = \frac{1}{j!} 2^{j(j+1)/2} up(-1 + 2^{-(k-j)}); j = 0, 1, \dots, k; k = 1, 2, \dots, \infty. \quad (5)$$

Calculation of the $up(-1 + 2^{-r}) ; r \in [0, \infty]$ in binary-rational points (Eq. 5), as well as all details regarding the calculation of the function $up(x)$ values, are provided in [Gotovac and Kozulić (1999)] and [Gotovac and Kozulić (2002)]. The argument $(x - 0, p_1 \dots p_k)$ in Eq. 4 is the difference between the real value of coordinate x and its binary form in k bits, where $p_1 \dots p_k$ are digits, 0 or 1, of the binary representation of the x coordinate. Therefore, the accuracy of the x coordinate computation, and, thus the accuracy of the $up(x)$ function at an arbitrary point, depends on machine accuracy.

From Eq. 2, it can be seen that the derivatives of the $up(x)$ function can be calculated simply from the values of the function itself. The general expression for the derivative of the m th degree is

$$up^{(m)}(x) = 2^{C_{m+1}^2} \sum_{k=1}^{2^m} \delta_k up(2^m x + 2^m + 1 - 2k), \quad m \in N \tag{6}$$

where $C_{m+1}^2 = m(m+1)/2$ is the binomial coefficient and δ_k are the coefficients with value ± 1 , according to the recursive formulas $\delta_{2k-1} = \delta_k, \delta_{2k} = -\delta_k, k \in N, \delta_1 = 1$. It can be observed that the derivatives consist of the $up(x)$ function compressed to an interval of 2^{-m+1} length, with ordinates extended by the $2^{C_{m+1}^2}$ factor, see Fig. 1.

The $Fup_n(x)$ function satisfies the following differential-functional equation:

$$Fup_n'(x) = 2 \sum_{k=0}^{n+2} \left(C_{n+1}^k - C_{n+1}^{k-1} \right) Fup_n(x) (2x - 2^{-n-1}k + 2^{-n-2}(n+2)) \tag{7}$$

where n is the Fup order. Index n also denotes the highest degree of the polynomial that can be expressed exactly as a linear combination of $n + 2$ $Fup_n(x)$ basis functions, uniformly displaced by a characteristic interval 2^{-n} .

For $n = 0, Fup_0(x) = up(x)$, since $Fup_n(x)$ and its derivatives can be calculated using a linear combination of displaced $up(x)$ functions instead of using their Fourier transforms:

$$Fup_n(x) = \sum_{k=0}^{\infty} C_k(n) up \left(x - 1 - \frac{k}{2^n} + \frac{n+2}{2^{n+1}} \right) \tag{8}$$

where $C_0(n) = 2^{C_{n+1}^2} = 2^{n(n+1)/2}$. In turn, $C_k(n) = C_0(n) \cdot C'_k(n)$, where a recursive formula is used for calculating auxiliary coefficients $C'_k(n)$:

$$C'_0(n) = 1, \text{ when } k = 0; \text{ i.e., when } k > 0$$

$$C'_k(n) = (-1)^k C_{n+1}^k - \sum_{j=1}^{\min\{k; 2^{n+1}-1\}} C'_{k-j}(n) \cdot \delta_{j+1} \tag{9}$$

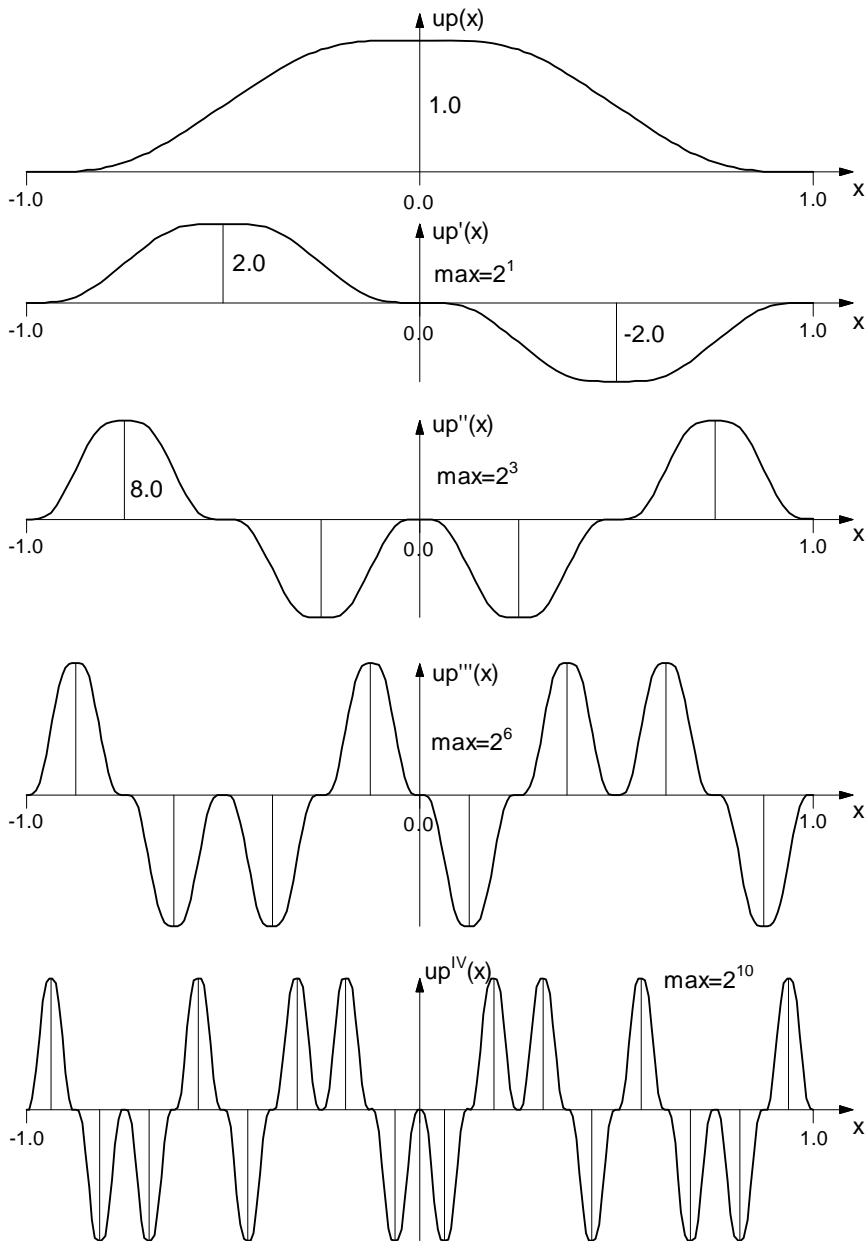


Figure 1: Function $up(x)$ and its first four derivatives

The $Fup_n(x)$ is defined over the compact support $[-(n+2) 2^{-n-1}; (n+2) 2^{-n-1}]$. Fig. 2 shows the $Fup_2(x)$ function and its first three derivatives, which are used in this paper.

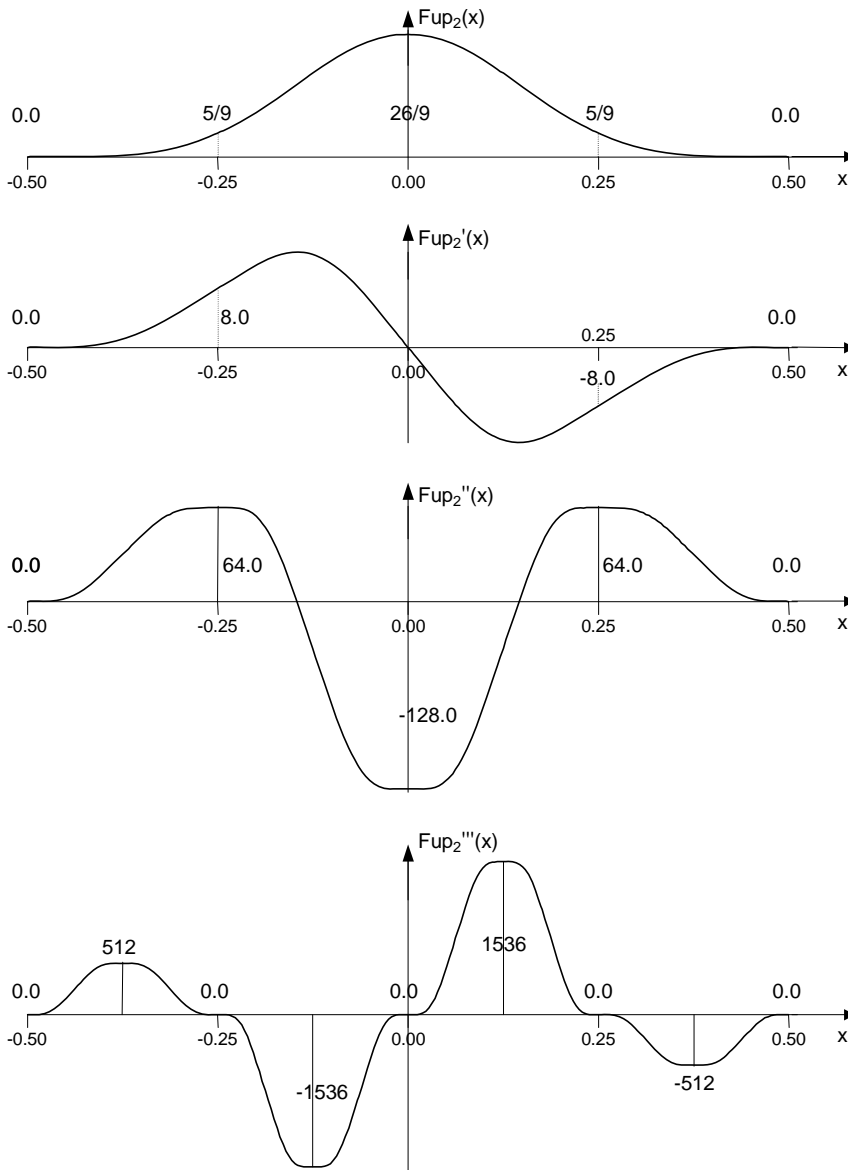


Figure 2: Function $Fup_2(x)$ and its first three derivatives

The basis function for numerical analyses of two-dimensional problems is obtained from the Cartesian product of two one-dimensional Fup functions defined for each direction:

$$Fup_n(x, y) = Fup_n(x) \cdot Fup_n(y). \quad (10)$$

Calculations of all required derivatives of the function $Fup_n(x, y)$ can be written in an analogue form. Fig. 3 gives an axonometric presentations of basis function $Fup_2(x, y)$ and its partial derivatives.

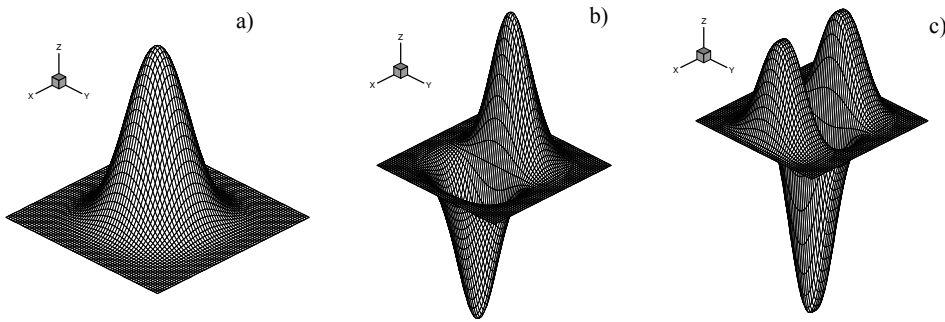


Figure 3: a) $Fup_2(x, y)$; b) $\frac{\partial Fup_2(x, y)}{\partial x}$; c) $\frac{\partial^2 Fup_2(x, y)}{\partial x^2}$

3 Equations of elastic and elasto-plastic torsion problem

The elastic torsion of a bar is a classical problem in the theory of elasticity [Timoshenko and Goodier (1961); Lurie (1970)]. This problem may be formulated in terms of the Dirichlet boundary value problem of the Poisson equation:

$$\frac{\partial^2 \Phi(x, y)}{\partial x^2} + \frac{\partial^2 \Phi(x, y)}{\partial y^2} = -2G\vartheta; \quad \Phi|_{\Gamma} = 0 \quad (11)$$

where $\Phi(x, y)$ is the stress function, G is the shear modulus, while ϑ is the angle of twist per unit length of a bar. Shear stress components are determined according to the following expressions:

$$\tau_{xz} = \partial\Phi/\partial y; \quad \tau_{yz} = -\partial\Phi/\partial x. \quad (12)$$

Torsion rigidity of the cross-section for $\vartheta = 1$ is the double volume under the surface of the stress function Φ :

$$C_t = 2 \iint \Phi \, dx \, dy. \quad (13)$$

In case of a cross-section with multiple boundary, unknown constant values of the stress function at inner boundaries Γ_i are determined based on the theorem on circulation of shear stresses. The following condition must be satisfied at each boundary of the opening:

$$-\int_{\Gamma_i} \frac{\partial \Phi}{\partial n_i} d\Gamma = 2G \vartheta A_i, \quad i = 1, 2, \dots, n \quad (14)$$

where A_i is the area of each opening, n_i is the normal to the inner boundary Γ_i , while n is the number of openings.

The material starts to deform plastically when the resulting shear stress in a point reaches a critical value τ_Y . Then, the Poisson equation is satisfied in elastic part of the domain while the yielding criterion [Hill (1985)]:

$$\left(\frac{\partial \Phi}{\partial x}\right)^2 + \left(\frac{\partial \Phi}{\partial y}\right)^2 = \tau_Y^2 \quad (15)$$

is satisfied in its plastic part. The greatest value of the torsion moment occurs when the entire cross-section is plasticized. It is the limit torsion moment M_{pl} . Elasto-plastic analyses includes determination of the angle of twist ϑ at which plasticization begins as well as monitoring of the expansion of plastic zones until limit moment M_{pl} is reached.

Numerical analysis of the given problem is performed by incremental-iterative procedure as follows:

1. In the first incremental step for an elastic state with the given rotation angle ϑ_1 , values of the stress function Φ and C_t of the cross-section are calculated.
2. In the next incremental step, increase of load $\Delta\vartheta$ is added i.e. $\vartheta_k = \vartheta_{k-1} + \Delta\vartheta$.
3. Increase of the stress function $\Delta\Phi$ is calculated. So, total values of the stress function are $\Phi_k = \Phi_{k-1} + \Delta\Phi$. For such stress state, torsion moment M_{calc} is calculated.
4. A control of plastic yielding is made by using the resulting shear stress τ . If $\tau < \tau_Y$ in all points of the cross-section, the procedure continues with the next load increment. If in some points $\tau \geq \tau_Y$, iterations within the current incremental step are performed.
5. In the points where plasticization occurred, values of the stress function return to a limiting value Φ_{red} .

6. For such reduced stress function Φ_{red} , torsion moment M_{ep} of partially plasticized cross-section is calculated and residual moment of torsion is $\Delta M = M_{calc} - M_{ep}$.
7. Elastic part of the cross-section is loaded with a residual moment of torsion, namely with the equivalent angle of twist $\Delta \vartheta_{ekv}$.
8. Iterative procedure is repeated until $\Delta M \cong 0$. Then, the next load increment follows.
9. Incremental-iterative procedure ends when $M_{calc} \geq M_{pl}$.

The basic yield criterion $\tau = \tau_Y$ is not numerically favorable for calculating values of the stress function Φ and residual load $\Delta \vartheta_{ekv}$ when the cross-section is partially plasticized. Therefore, we modified the basic yield criterion into the criterion of testing the stress function Φ where the idea of R-functions is used for the determination of its limit values. R-functions are the real functions with the real continuous arguments, which at the same time have several properties of Boole's functions [Rvachev (1982)].

Limiting values Φ_{pl} are values of the stress function when the entire cross-section is plasticized. Then, the stress function Φ forms a surface with the constant inclination covering the entire cross-section.

E.g. for a polygonal area Ω , Fig. 4, R-function is sought in the form $\omega(x, y) = \omega_1 \wedge \omega_2 \wedge \omega_3 \wedge \omega_4$ where $\omega(x, y) \geq 0, \forall (x, y) \in \bar{\Omega}; \omega(x, y) < 0, \forall (x, y) \notin \bar{\Omega}$.

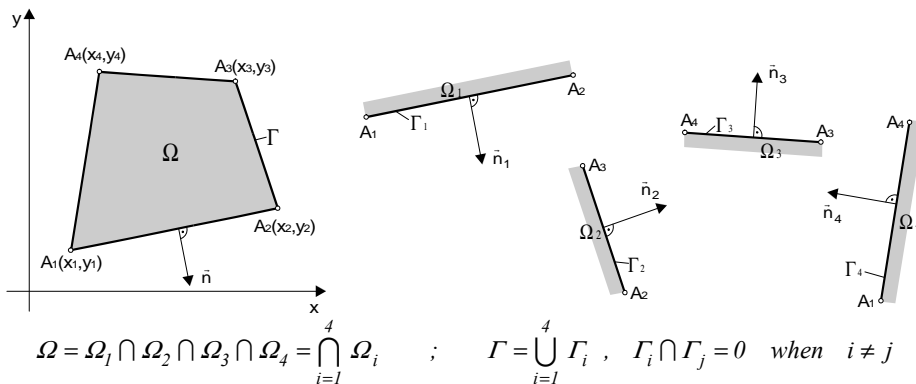


Figure 4: Determining of a polygonal area with the R-function

Each component of the sought R-function must satisfy conditions:

$$\omega_i|_{\Gamma_i} = 0; \quad \frac{\partial \omega_i}{\partial n_i}|_{\Gamma_i} = \tau_Y \tag{16}$$

and, thus, has the following form:

$$\omega_i(x, y) = \tau_Y \cdot \frac{-x(y_{i+1} - y_i) + y(x_{i+1} - x_i) - x_{i+1}y_i + x_iy_{i+1}}{\sqrt{(y_{i+1} - y_i)^2 + (x_{i+1} - x_i)^2}} \geq 0 \tag{17}$$

By analogy, when the cross-section side is a segment of circular arc, see Fig. 5, function $\omega_i(x, y)$ has the following form:

$$\omega_i(x, y) = \text{Sign}(P_\Delta) \cdot \left\{ \tau_Y \cdot \left(R - \sqrt{(x - x_c)^2 + (y - y_c)^2} \right) \right\} \geq 0 \tag{18}$$

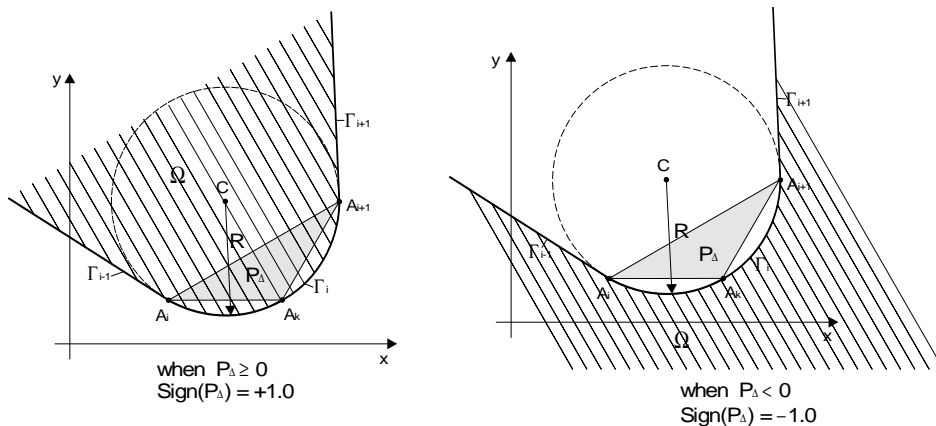


Figure 5: Determining of the R-function component for the boundary segment in the form of circular arc

In the cross-section point with coordinates (x, y) for a convex domain, value Φ_{pl} is determined as $\Phi_{pl} = \min \{ \omega_1, \omega_2, \dots, \omega_n \}$ where n is the number of sides on the domain boundary. If the angle between two adjacent sides $i, i + 1$ is greater than 180° (concave corner), bigger value is selected between $\omega_i(x, y)$ and $\omega_{i+1}(x, y)$.

4 Solution procedure by the Fup Collocation Method (FCM)

Approximate solution of the stress function $\Phi(x, y)$ in Eq.11 is assumed in the form of linear combination of basis functions $Fup_2(x, y)$. A system of equations

is formed by the collocation method where differential equation of the problem is satisfied in collocation points of a closed domain while boundary conditions are satisfied exactly at the domain boundary. It is known that functionality of the collocation method depends on the selection of basis functions and collocation points. Prenter (1989) proved the stability of numerical procedure with the spline functions when collocation is performed in so-called natural knots. He developed proofs for existence and uniformity of the solution and error estimate. Since Fup functions can be regarded as splines of an infinite degree, it can be shown that for them it is also optimal to perform collocation in natural knots of basis functions, i.e. vertices of basis functions situated in a closed domain such as e.g. for the base in x -direction formed by functions $Fup_2(x)$ shown in Fig. 6.

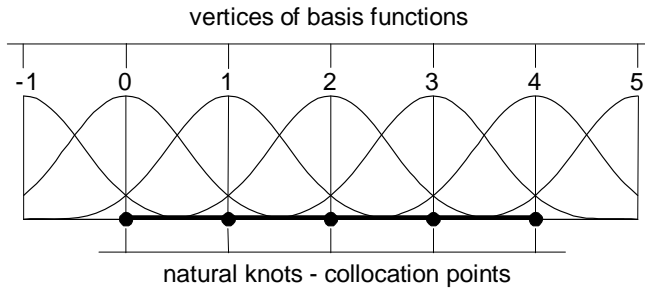


Figure 6: Collocation points of the base formed by $Fup_2(x)$ functions

This selection of collocation points provides the simplest numerical procedure, banded collocation matrix is obtained, which is diagonally dominant and thus well conditioned. This selection also implies uniformly distributed nodes set in each coordinate direction.

4.1 Analyses of rectangular domains

Approximate solution base is formed on the unit virtual domain defined in the system (ξ, η) according to a scheme shown in Fig. 7.

For rectangular cross-section of $a \times b$ dimensions, differential equation of the problem and boundary condition from Eq.11 can be written in the system (ξ, η) as:

$$\frac{1}{a^2} \frac{\partial^2 \Phi(\xi, \eta)}{\partial \xi^2} + \frac{1}{b^2} \frac{\partial^2 \Phi(\xi, \eta)}{\partial \eta^2} = -2G\vartheta; \quad 0 \leq \xi \leq 1, \quad 0 \leq \eta \leq 1, \quad (19)$$

$$\Phi(\xi, \eta) = 0 \quad \text{for } \xi = 0, \xi = 1, \eta = 0, \eta = 1. \quad (20)$$

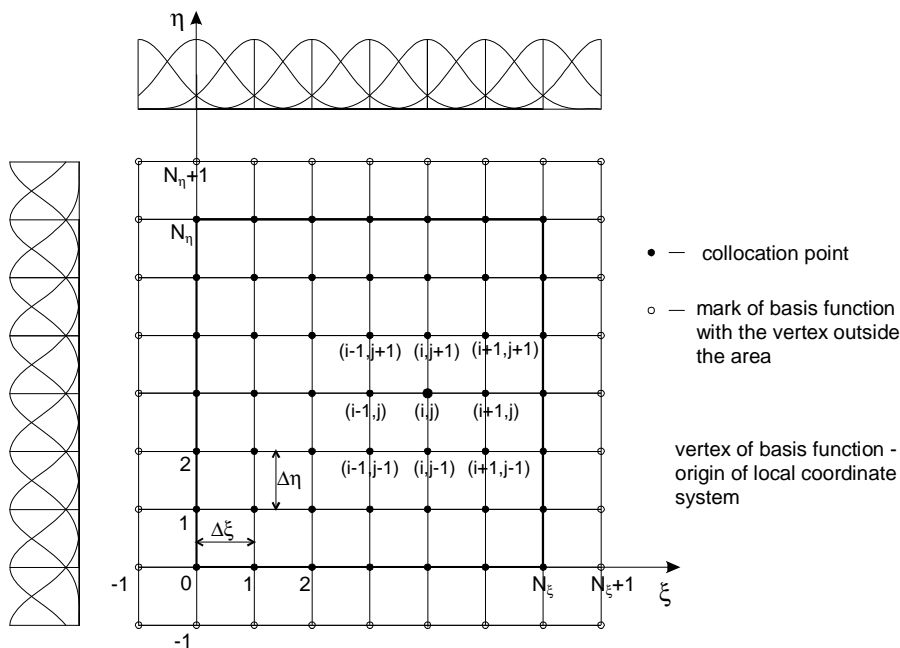


Figure 7: Distribution of basis functions on the unit virtual domain

Collocation is performed in $(N_\xi + 1) \times (N_\eta + 1)$ equidistant points, while basis functions with vertices outside the domain, see Fig. 7, are retained so the basis functions set can be complete. Governing equation (19) is satisfied in all collocation points of the domain except in corners:

$$\sum_{i=-1}^{N_\xi+1} \sum_{j=-1}^{N_\eta+1} C_{ij} \left(\frac{1}{a^2} \frac{\partial^2 F_{ij}(\xi, \eta)}{\partial \xi^2} + \frac{1}{b^2} \frac{\partial^2 F_{ij}(\xi, \eta)}{\partial \eta^2} \right) = -2G\vartheta, \quad (21)$$

boundary condition (20) is satisfied in all collocation points of the domain sides:

$$\sum_{i=-1}^{N_\xi+1} \sum_{j=-1}^{N_\eta+1} C_{ij} \cdot F_{ij}(\xi, \eta) = 0, \quad (22)$$

while three more conditional equations are satisfied in corners:

$$\begin{aligned} \sum_{i=-1}^{N_{\xi}+1} \sum_{j=-1}^{N_{\eta}+1} \frac{1}{a^2} C_{ij} \frac{\partial^2 F_{ij}(\xi, \eta)}{\partial \xi^2} &= 0 \\ \sum_{i=-1}^{N_{\xi}+1} \sum_{j=-1}^{N_{\eta}+1} \frac{1}{b^2} C_{ij} \frac{\partial^2 F_{ij}(\xi, \eta)}{\partial \eta^2} &= 0 \quad . \\ \sum_{i=-1}^{N_{\xi}+1} \sum_{j=-1}^{N_{\eta}+1} \frac{1}{a^2 b^2} C_{ij} \frac{\partial^4 F_{ij}(\xi, \eta)}{\partial \xi^2 \partial \eta^2} &= 0 \end{aligned} \quad (23)$$

In the equation system (21)-(23), N_{ξ} and N_{η} denote numbers of partitions of a unit domain in directions ξ and η respectively; i and j are counters of the basis functions in ξ i.e. η directions, while $F_{ij}(\xi, \eta)$ is the basis function $Fup_2(\xi, \eta)$ with the vertex at the point (i, j) . Depending on the number of partitions, function $Fup_2(\xi, \eta)$ support is condensed to $(4\Delta\xi \times 4\Delta\eta)$; $\Delta\xi = 1/N_{\xi}$, $\Delta\eta = 1/N_{\eta}$. Partial derivatives values of basis functions in Eqs. (21)-(23) are determined according to the following expression:

$$\frac{\partial^{(m+n)} F_{ij}(\xi, \eta)}{\partial \xi^m \partial \eta^n} = \left(\frac{1}{4\Delta\xi} \right)^m \cdot \left(\frac{1}{4\Delta\eta} \right)^n \cdot Fup_2^{(m+n)} \left(\frac{1}{4\Delta\xi} \xi - \frac{i}{4}, \frac{1}{4\Delta\eta} \eta - \frac{j}{4} \right). \quad (24)$$

Since the function $Fup_2(\xi, \eta)$ is a finite function with the support consisting of 4×4 characteristic intervals (see Fig. 2), the solution function value at collocation point (i, j) can be approximated by linear combination in the following form:

$$\Phi(\xi_i, \eta_j) = \sum_{k=i-1}^{i+1} \sum_{l=j-1}^{j+1} C_{kl} \cdot F_{kl}(\xi_i, \eta_j). \quad (25)$$

Values of all other basis functions at the point (i, j) are equal to zero. Therefore, a support domain of the point (i, j) is nine. In such a way, banded matrix of the system is obtained.

4.2 Analyses of curvilinear domains

FCM can be applied successfully to curvilinear domains, too.

Parametric form is extremely adequate for description of surfaces and, using the

Coons formulation [Yamaguchi (1988)], can be written in the following form:

$$P(\xi, \eta) = [(1-\xi) \quad \xi] \begin{bmatrix} Q(0, \eta) \\ Q(1, \eta) \end{bmatrix} + [Q(\xi, 0) \quad Q(\xi, 1)] \begin{bmatrix} 1-\eta \\ \eta \end{bmatrix} - [(1-\xi) \quad \xi] \begin{bmatrix} Q(0, 0) & Q(0, 1) \\ Q(1, 0) & Q(1, 1) \end{bmatrix} \begin{bmatrix} 1-\eta \\ \eta \end{bmatrix} \tag{26}$$

where $Q(0, 0)$, $Q(0, 1)$, $Q(1, 0)$ and $Q(1, 1)$ are position vectors at the four corners while $Q(\xi, 0)$, $Q(\xi, 1)$, $Q(0, \eta)$ and $Q(1, \eta)$ are four boundary curves, see Fig. 8. Changing the parameters ξ and η in equal steps on the interval $[0, 1]$, using Eq. 26, equidistant collocation points within the given domain are obtained.

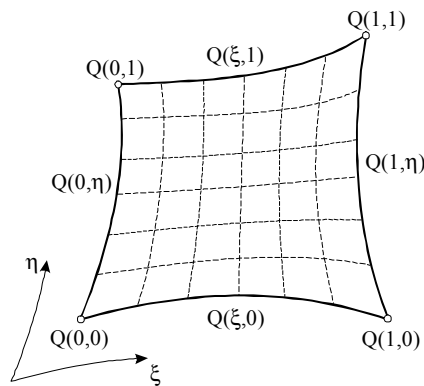


Figure 8: A Coons surface patch

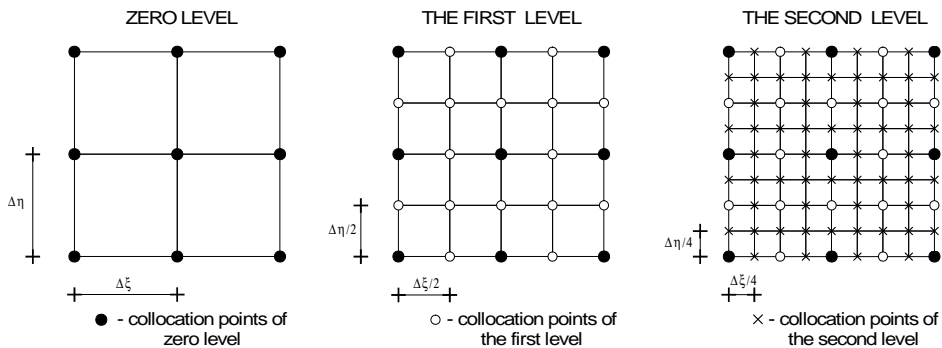


Figure 9: Hierarchic expansion of a vector space of the functions $Fup_2(\xi, \eta)$

Thus, for curvilinear domains, partial differential equation of the torsion problem, Eq.11, has the following collocation form:

$$\sum_{i=-1}^{N_\xi+1} \sum_{j=-1}^{N_\eta+1} C_{ij} \cdot \left[F_{XX} \frac{\partial^2 F_{ij}(\xi, \eta)}{\partial \xi^2} + F_{XE} \frac{\partial^2 F_{ij}(\xi, \eta)}{\partial \xi \partial \eta} + F_{EE} \frac{\partial^2 F_{ij}(\xi, \eta)}{\partial \eta^2} + F_X \frac{\partial F_{ij}(\xi, \eta)}{\partial \xi} + F_E \frac{\partial F_{ij}(\xi, \eta)}{\partial \eta} \right] = -2G\vartheta \tag{27}$$

where:

$$F_{XX} = \left(\frac{\partial \xi}{\partial x} \right)^2 + \left(\frac{\partial \xi}{\partial y} \right)^2 ; \quad F_{EE} = \left(\frac{\partial \eta}{\partial x} \right)^2 + \left(\frac{\partial \eta}{\partial y} \right)^2 ;$$

$$F_{XE} = 2 \cdot \left(\frac{\partial \xi}{\partial x} \frac{\partial \eta}{\partial x} + \frac{\partial \xi}{\partial y} \frac{\partial \eta}{\partial y} \right)$$

$$F_X = \frac{\partial \xi}{\partial x} \frac{\partial}{\partial \xi} \left(\frac{\partial \xi}{\partial x} \right) + \frac{\partial \eta}{\partial x} \frac{\partial}{\partial \eta} \left(\frac{\partial \xi}{\partial x} \right) + \frac{\partial \xi}{\partial y} \frac{\partial}{\partial \xi} \left(\frac{\partial \xi}{\partial y} \right) + \frac{\partial \eta}{\partial y} \frac{\partial}{\partial \eta} \left(\frac{\partial \xi}{\partial y} \right)$$

$$F_E = \frac{\partial \xi}{\partial x} \frac{\partial}{\partial \xi} \left(\frac{\partial \eta}{\partial x} \right) + \frac{\partial \eta}{\partial x} \frac{\partial}{\partial \eta} \left(\frac{\partial \eta}{\partial x} \right) + \frac{\partial \xi}{\partial y} \frac{\partial}{\partial \xi} \left(\frac{\partial \eta}{\partial y} \right) + \frac{\partial \eta}{\partial y} \frac{\partial}{\partial \eta} \left(\frac{\partial \eta}{\partial y} \right) \tag{28}$$

Partial derivatives of elements of the inverse mapping matrix in expressions of Eq. 28 are determined by derivations of parametric equations of a surface (Eq. 26), while partial derivatives of the basis functions are determined according to Eq. 24.

4.3 Multilevel approach

Hierarchic expansion of an approximate solution base is realized by an algorithm in which new functions, which are all images of the same mother basis function, are added to the base of an initial solution, but displaced and compressed or stretched in comparison with the initial base.

When $(N_\xi + 3) \times (N_\eta + 3)$ basis functions mutually displaced by $\Delta\xi$ in one and $\Delta\eta$ in the other coordinate direction are selected, as shown in Fig. 7, then the selected base is at the “zero level” of approximation. At the first level, functions $Fup_2(\xi, \eta)$ are added, displaced by $\Delta\xi/2 ; \Delta\eta/2$ in reference to the functions of zero level, and compressed to a support length $(2\Delta\xi) \times (2\Delta\eta)$. At the second level, added basis functions are displaced by $\Delta\xi/4 ; \Delta\eta/4$ in reference to “zero level” with the support length $(\Delta\xi \times \Delta\eta)$, which is 1/4 of the length of basis function support at zero level. At higher levels of approximation, the base is built by analogy. Fig. 9 shows the distribution of collocation points, in which vertices of basis functions are

at the zero, first and second levels of approximation. Compression of the functions to 1/2 of the support from the preceding level is the consequence of basic properties of atomic functions [Gotovac and Kozulić (1999)].

Numerical tests [Kozulić and Gotovac (2000)] for different densities of collocation points showed that it is sufficient to satisfy the boundary conditions with basis functions of zero level while basis functions of higher levels correct the solution.

5 Numerical examples

5.1 Torsion of a prismatic bar with a square cross-section

Elastic torsion of a bar with a square cross-section shown in Fig. 10 is analyzed for $\vartheta = 1$ by FCM. An analytic solution for this shape of a cross-section is given by Timoshenko and Goodier (1961). The effect of hierarchic increasing a number of basis functions is illustrated. Fig. 11 shows the convergence diagrams of numerical solutions for torsion rigidity value when number of basis functions increases at zero level only, and when approximate solution base is expanded with basis functions of the first and second levels. It can be observed that with the same total number of basis functions, much better numerical solution is obtained if multilevel approach is applied.

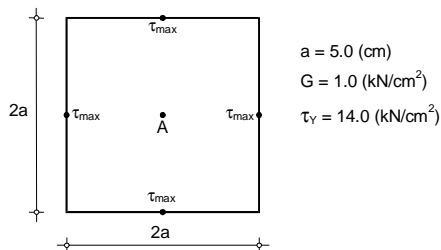


Figure 10: Square cross-section

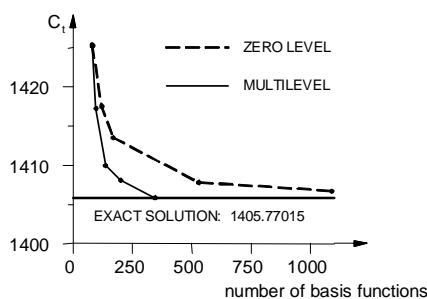


Figure 11: Convergence diagrams for C_t

Elasto-plastic behaviour of the cross section was analyzed both with numerical model based on the Finite Element Method and numerical model based on the Fup Collocation Method. Assuming that the bar is not deformed until the yielding limit is exceeded, limit torsion moment can be determined according to expression $(8\tau_y a^3)/3$ and, for values given in Fig. 10, equals $M_{pl} = 4666.667 \text{ kNcm}$. Numerical model by the FEM uses eight-node isoparametric finite elements with

Lagrange polynomials of the 2nd degree as basis functions. Tab. 1 shows the comparison of numerical values obtained by these two methods for the torsion moment and the appurtenant angle of twist ϑ at which the full plasticization of a cross-section is registered.

Table 1: Comparison of numerical results obtained by FEM and FCM

	FEM: number of finite elements			FCM: number of collocation points			Exact values
	25	100	625	11×11	21×21	51×51	
M_{pl}	4480.01	4619.99	4659.25	4620.00	4655.00	4664.80	4666.67
ϑ_{pl}	4.58	7.72	17.91	40.73	141.17	1475.37	∞

In real, indefinitely large angle of twist is required to obtain full plasticization of the cross-section. So, from the results given in Tab. 1 one can observed that numerical solution obtained by the FCM described the real elasto-plastic behavior of a bar better than the model by the FEM. In the moment when numerical models register full plasticization of the cross-section and interrupt numerical procedure, model by the FCM gives the limiting values of the stress function Φ in all calculation points of the domain while this can never be achieved by the FEM.

Gradual plasticization of the cross section with the increase in the angle ϑ obtained by Fup Collocation Method is given in Fig. 12. Plastic zones first occur at the domain boundary, and then spread towards the inside. We started calculation with initial density of 11 collocation points in each coordinate direction. When collocation points are detected in which plasticity criterion is satisfied, number of basis functions is increased only in plastic part of the cross-section according to a scheme given in Fig. 9, while in elastic core initial density at zero level is retained. Thus, movement of the plastic zone boundary is successfully simulated until elastic core completely disappears.

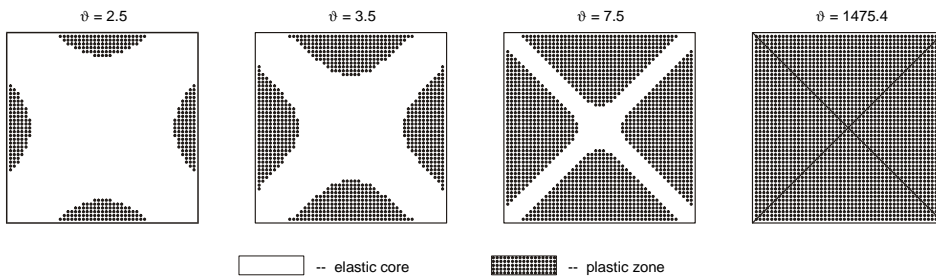


Figure 12: Plastic yielding of a bar with a square cross-section

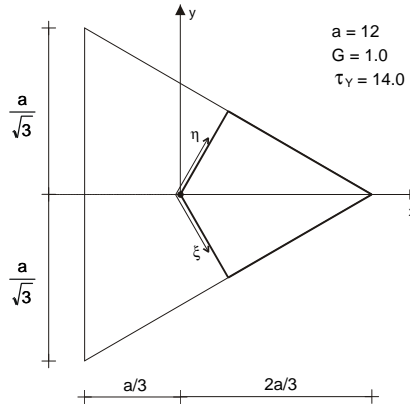


Figure 13: Triangular cross-section

5.2 Plastic yielding of a bar with a triangular cross-section

Plastic yielding of a bar with a triangular cross-section is analyzed by the FCM using the conditions of symmetry as shown in Fig. 13.

Theoretical value of the limit torsion moment is equal to the double volume under the stress function surface for a completely plastic cross-section:

$$M_{pl} = \frac{2\sqrt{3}}{27} \cdot \tau_Y \cdot a^3 \quad (29)$$

and, for given values of τ_Y and a , is $M_{pl} = 3103.835$. Fig. 14 shows isolines of stress function Φ in the plan and shapes of the stress function over the cross-section ranging from elastic to completely plastic state.

Tab. 2 gives a convergence of numerical solutions. N denotes total number of the $Fup_2(\xi, \eta)$ basis functions per each coordinate direction obtained by a hierarchic expansion of the approximate solution base until plastic failure is registered.

Table 2: Convergence of numerical solutions for triangular cross-section

	N=4	N=10	N=20	N=50	Exact
M_{pl}	2888.599	3066.411	3094.227	3102.273	3103.835
ϑ_{pl}	196.102	240.026	7602.955	44788.654	∞

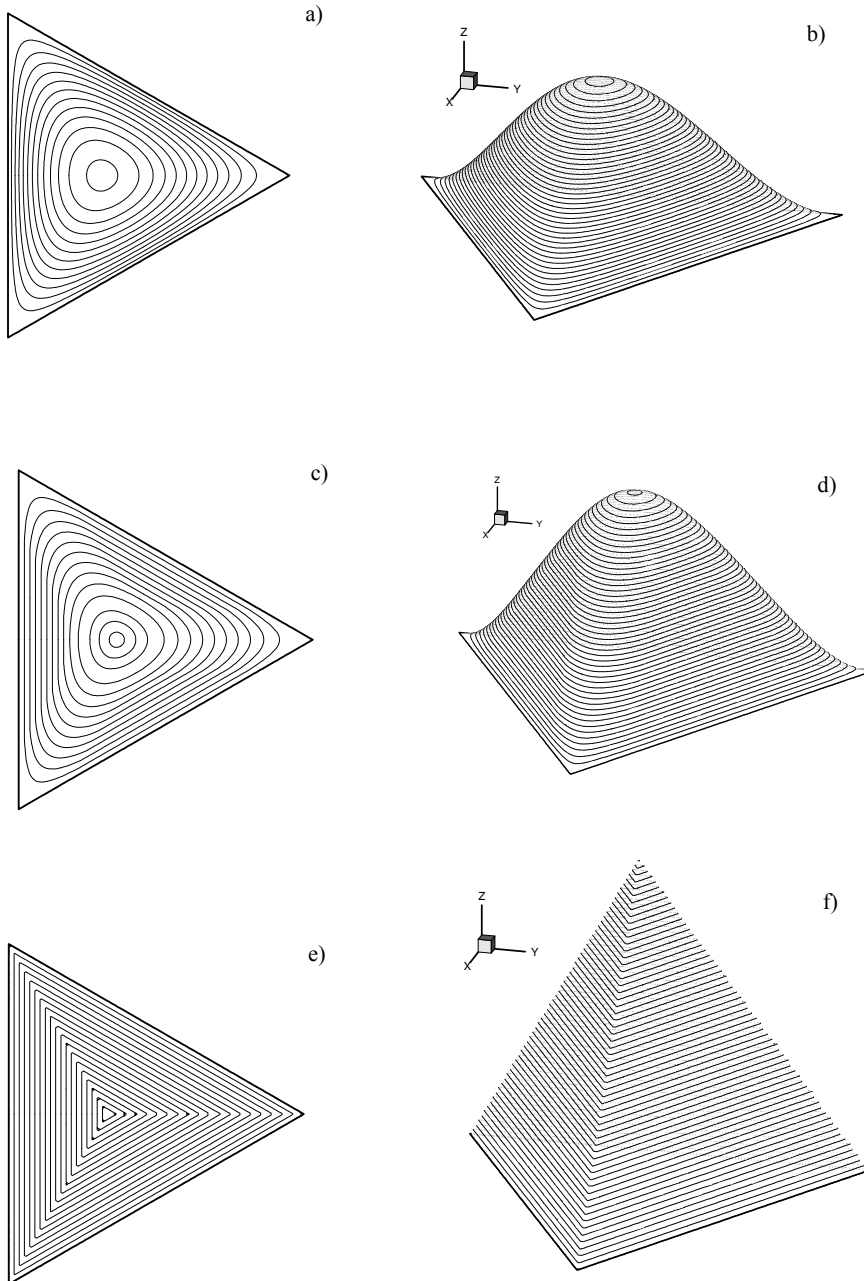


Figure 14: Plastic yielding of a triangle cross-section obtained by FCM: a), b) for $\vartheta = 2.0$; c), d) for $\vartheta = 4.1$; e), f) for $\vartheta = 44788.6$

5.3 Cross-section in the form of an eccentric ring

Elastic and elasto-plastic analyses of a bar with a cross-section in the form of an eccentric ring, shown in Fig. 15, were made by FCM. An analytic solution exists for this shape of a cross-section [Lurie (1970)].

A real domain of a cross-section is mapped into the virtual unit domain using Eq. 26 where sides (1) and (2), see Fig. 16, are described using the parametric equations of a circle; sides (3) and (4) overlap in a real domain.

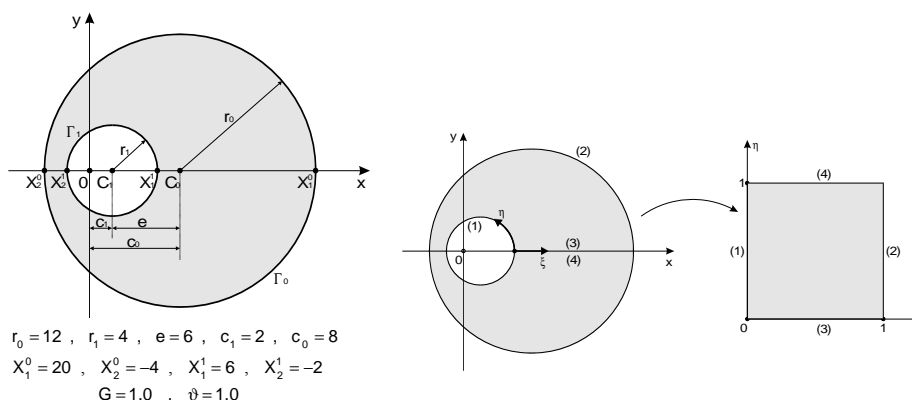


Figure 15: Cross-section geometry Figure 16: Mapping of the considered domain

Convergence of torsion rigidity value C_t and stress function value Φ on the inner boundary Γ_1 with an increase in the number of collocation points is given in Tab. 3. Fig. 17 shows the stress function surface obtained by the Fup Collocation Method for $\vartheta = 1.0$.

Table 3: Numerical results of elastic analyses depending on N_ξ and N_η

Number of coll. points: ($N_\xi + 1$) \times ($N_\eta + 1$)	$\Phi _{\Gamma_1}$	$\frac{\Phi - \Phi_{exact}}{\Phi_{exact}}$	C_t	$\frac{C_t - C_{t exact}}{C_{t exact}}$
$N_\xi = 10, N_\eta = 20$	41.387	5.32 %	28345.72	2.57 %
$N_\xi = 20, N_\eta = 40$	40.279	2.50 %	27976.24	1.24 %
$N_\xi = 50, N_\eta = 100$	39.649	0.90 %	27768.75	0.48 %
$N_\xi = 100, N_\eta = 200$	39.445	0.38 %	27701.30	0.24 %
Exact solution [Lurie (1970)]	39.297	–	27634.63	–

For the purpose of elasto-plastic analysis, twist angle ϑ increases to the full plastic

yielding. Theoretical value of the limit torsion moment M_{pl} for the yield stress value $\tau_Y = 14.0$, is 37708.746.

Fig. 18 shows surface shapes and isolines of the stress function Φ obtained for different load increments, from fully elastic to fully plastic state.

Tab. 4 gives numerical values of torsion moment and the appurtenant angle of twist ϑ at which the full plasticization of a cross-section is registered for different densities of collocation points.

Table 4: Convergence of numerical results for elasto-plastic analysis

Num. of coll. points ($N_\xi+1$) \times ($N_\eta+1$)	$N_\xi = 6$ $N_\eta = 12$	$N_\xi = 10$ $N_\eta = 20$	$N_\xi = 20$ $N_\eta = 40$	$N_\xi = 50$ $N_\eta = 100$	ANALYTIC VALUES
M_{pl}	36675.289	37380.531	37619.290	37694.477	37708.746
ϑ_{pl}	12.651	123.014	361.527	999088.787	∞

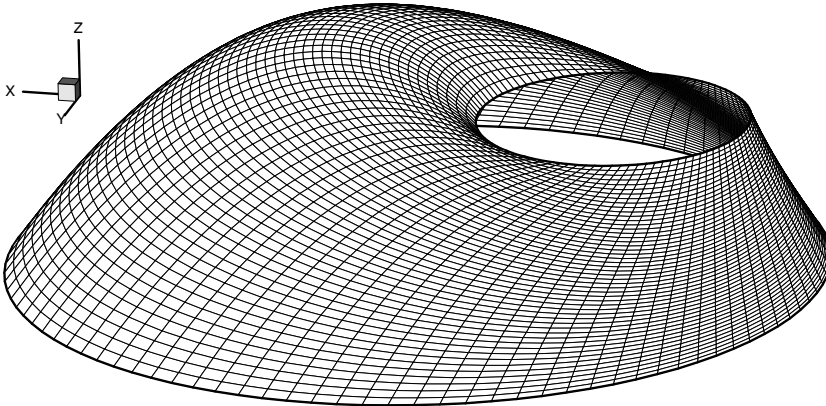


Figure 17: Stress function surface $\Phi(x, y)$ for elastic state of a bar

6 Conclusions

Numerical model for elasto-plastic analyses of a prismatic bar subjected to torsion is described in this work. It enables analyses of bars with cross-sections of different shapes including a single and multiple boundary.

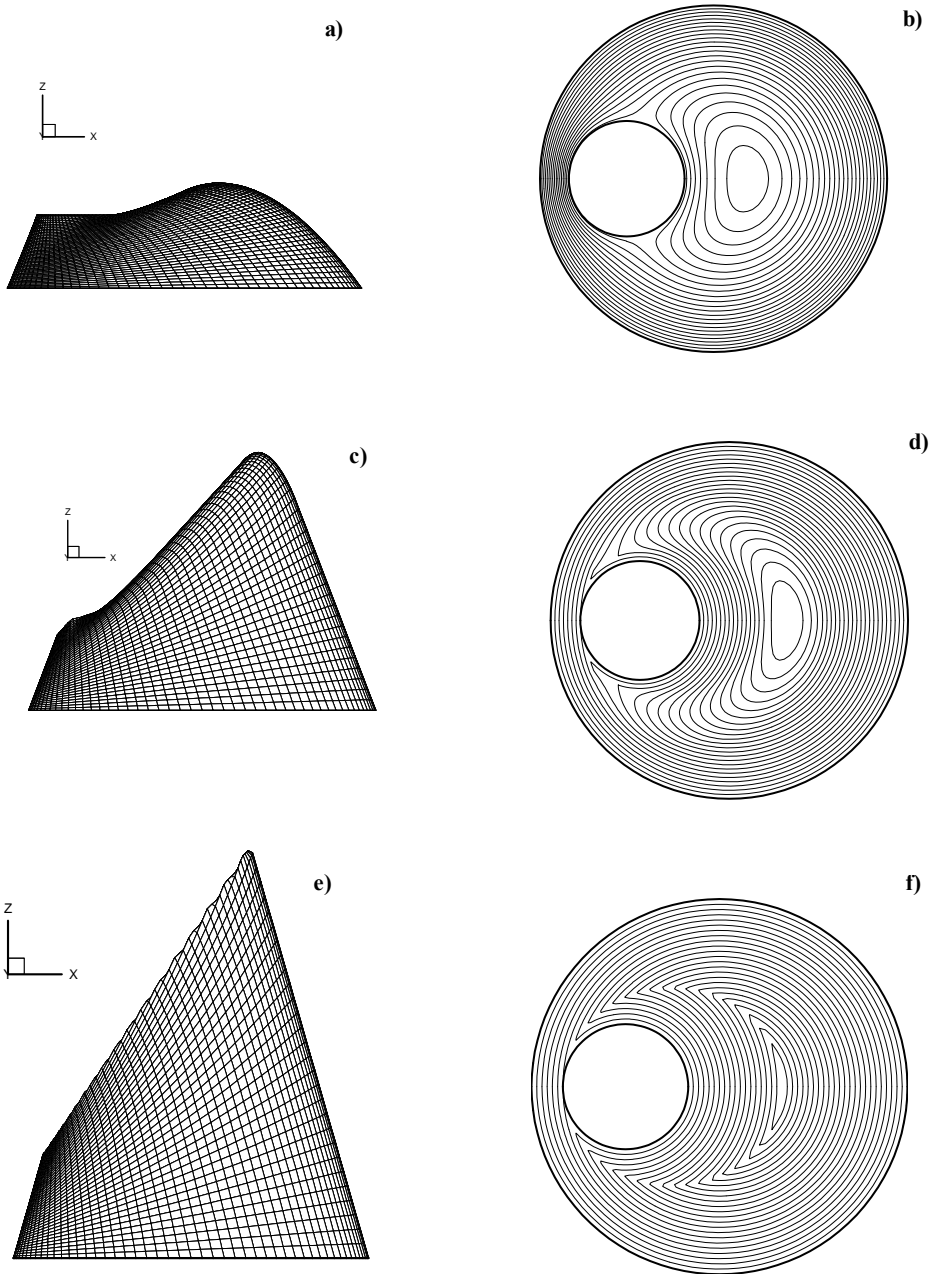


Figure 18: Plastic yielding of a cross-section in the form of an eccentric ring: a), b) for $\vartheta = 0.5$; c), d) for $\vartheta = 3.285$; e), f) for $\vartheta \rightarrow \infty$

The procedure is based on the use of atomic functions, particularly Fup basis functions, and collocation method. The basic yield criterion in elasto-plastic torsion problem i.e. that the resulting shear stress in a point is reached a critical value, is modified into the criterion of testing the stress function where the idea of R-functions is used for determination of its limit values. Hierarchic increase in the number of basis functions in the model provides a simple way to increase the accuracy of an approximate solution in places where plastic yielding occurs and also accelerates the convergence of incremental-iterative procedure. FCM can be applied successfully in the curvilinear domains by using the Coons formulation for parametric description of surfaces.

The numerical examples show that the new method efficiently simulates the real non-linear behavior of the structure by comparing with the exact solutions. More accurate results are attained with the FCM in comparison with the Finite Element Method which always records plastic failure before it really happens. In the Fup Collocation Method, the criterion of plasticity is tested in the same points for which the values of the solution function are calculated i.e. in collocation points. Thus, the numerical procedure with the FCM is stable until plastic failure occurs.

References

- Gotovac, B.; Kozulić, V.** (1999): On a selection of basis functions in numerical analyses of engineering problems. *Int. J. for Engineering Modelling*, vol. 12, no. 1-4, pp. 25-41.
- Hill, R.** (1985): *The Mathematical Theory of Plasticity*. Oxford University Press, New York.
- Kozulić, V.; Gotovac, B.** (2000): Numerical analyses of 2D problems using $Fup_n(x,y)$ basis functions. *Int. J. for Engineering Modelling*, vol. 13, no. 1-2, pp. 7-18.
- Kravchenko, V. F.; Rvachev, V. A.; Rvachev, V. L.** (1995): Mathematical methods for signal processing on the basis of atomic functions. *Radiotekhnika i Elektronika*, vol. 40, no. 9, pp. 1385-1406. (in Russian)
- Liu, C.-S.** (2007): Elastic Torsion Bar with Arbitrary Cross-Section Using the Fredholm Integral Equations. *CMC: Computers, Materials, and Continua*, vol. 5, no. 1, pp. 31-42.
- Lurie, A. I.** (1970): *Theory of Elasticity*. Nauka, Moskva.
- Prenter, P. M.** (1989): *Splines and Variational Methods*. John Wiley & Sons, New York.
- Rvachev, V. L.; Rvachev, V. A.** (1971): On a Finite Function. *DAN URSSR*, ser. A, no. 6, pp. 705-707.

Rvachev, V.L. (1982): *Theory of R-functions and their application*, (in Russian). Naukova dumka, Kiev.

Timoshenko, S.P.; Goodier, J.M. (1961): *Theory of Elasticity*. McGraw-Hill, New York.

Yamaguchi, F. (1988): *Curves and Surfaces in Computer Aided Geometric Design*. Springer-Verlag, Berlin.